Applied Catalysis B: Environmental 160–161 (2014) 1–9

Contents lists available at ScienceDirect

Applied Catalysis B: Environmental

journal homepage: www.elsevier.com/locate/apcatb

New insights into sulfur poisoning on a vanadia SCR catalyst under simulated diesel engine operating conditions

Yuanzhou Xi*, Nathan A. Ottinger, Z. Gerald Liu

Cummins Emission Solutions, 1801 US Hwy 51-138, Stoughton, WI 53589, United States

ARTICLE INFO

Article history:
Received 26 January 2014
Received in revised form 16 April 2014
Accepted 22 April 2014
Available online 6 May 2014

Keywords:
Vanadia SCR
Sulfur dioxide
Low temperature event
Deactivation
Kinetic analysis

ABSTRACT

Vanadia-based SCR (VSCR) catalysts can effectively remove NO_x (NO and NO_2) from diesel exhaust using urea hydrolysis produced NH_3 as a reductant. VSCR catalysts are often used because of their excellent sulfur tolerance. However, ammonium (bi)sulfate—which could form from the combination of SO_3 or H_2SO_4 with NH_3 when a diesel engine is operated at low load with high sulfur diesel fuel—can physically poison VSCR catalysts and lead to decreased NO_x conversion. In this study, the effects of 50 ppmv SO_2 on the catalytic performance of a state-of-the-art VSCR catalyst were investigated using a lab reactor under simulated diesel engine operating conditions. Experiments were performed to investigate two distinct real-world diesel aftertreatment temperature regimes: (1) typical diesel exhaust temperatures of 473–573 K, and (2) temperatures as low as 317 K to simulate engine start-up and shut-down. It was found that the presence of 50 ppmv SO_2 under SCR conditions at 473–573 K slightly increases NO_x conversion. On the other hand, temporarily cooling the catalyst temperature to 317 K in the presence of 50 ppmv SO_2 under SCR conditions leads to significant catalyst deactivation. Results from kinetic analysis, temperature programmed desorption (TPD), diffuse reflectance Fourier transform infrared spectroscopy (DRIFTS) and BET surface area measurements indicate the physical poisoning of VSCR catalysts due to the formation of ammonium sulfate species during the cooling process which significantly decreases the number of catalytic sites for SCR reaction. This work indicates that during low temperature events, simulating engine start-up and shut-down, SO_2 and NH_3 can combine and be oxidized to ammonium sulfate species which initiate progressive VSCR deactivation via physical poisoning.

© 2014 Elsevier B.V. All rights reserved.

1. Introduction

Increasing requirements for the reduction of NO_x emissions from mobile and stationary diesel engines are being enforced globally because NO_x has a significant impact on the environment and human health. The vanadia-based SCR catalyst (VSCR) is a proven technology for NO_x reduction using NH_3 as a reductant because of its high SCR reactivity, durability and tolerance for chemical poisoning by sulfur species. VSCR catalysts are widely used for Euro IV, V, and VI on-highway applications and are being proposed for U.S. Tier 4 Final and Euro Stage IV nonroad applications. Due to their robustness to chemical poisoning by sulfur species in diesel exhaust, VSCR catalysts can be utilized in regions where ultra-low sulfur diesel (ULSD) is not available [1]. However, ammonium (bi)sulfate, which could form in the presence of SO_3 and NH_3 at low exhaust temperatures, can physically block the catalyst surface and decrease NO_x reduction efficiency [2–6]. SO_3 can form via oxidation of SO_2 over the vanadia SCR catalyst, and engine out SO_x (SO_2 and SO_3) also contains a small fraction of less than 5% SO_3 [7,8]. The concentration of engine out SO_x is directly related to the air to fuel ratio and the sulfur content of diesel fuel as shown in Fig. 1. Ultra-low sulfur diesel with less than 15 ppmw (parts per million by weight) sulfur results in ~0.5 ppmv (parts per million by volume) engine out SO_x; diesel fuel with 1000–2000 ppmw sulfur leads to engine out SO_x of ~50 ppmv; several hundred ppmv SO_x can be present in the exhaust of marine diesel engines which may use diesel fuel with 0.1–3 wt.% (weight percent) sulfur [6].

Extensive research has been conducted to understand the effect of SO_2 on the NO_x reduction efficiency of VSCR catalysts. It was found that the presence of SO_2 during SCR reaction [9,10] or pretreatment with SO_2 [5] prior to SCR reaction can increase the reactivity of the vanadia-based SCR catalyst. On the other hand, Magnusson et al. reported that the presence of 500 ppmv SO_2 does not have a significant effect on the SCR reaction above 573 K and below 12 kh^{-1} space velocity, while at temperatures lower

* Corresponding author at: Cummins Emission Solutions, 1801 US Hwy 51-138, Stoughton, WI 53589, United States. Tel.: +1 608 873 2430; fax: +1 608 873 2409.
E-mail addresses: yuanzhou.xi@cummins.com, yx8f@virginia.edu (Y. Xi).

http://dx.doi.org/10.1016/j.apcatb.2014.04.037
0926-3373/© 2014 Elsevier B.V. All rights reserved.

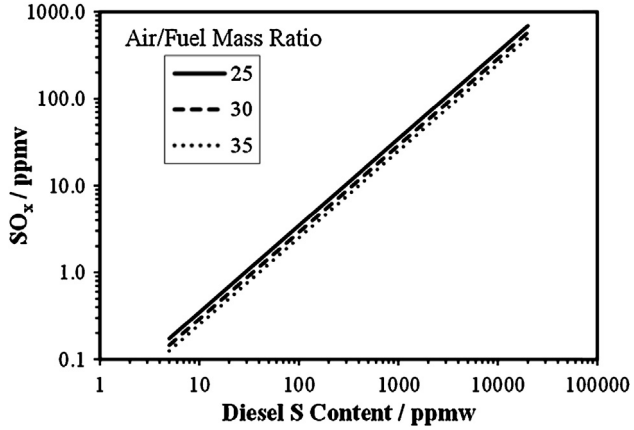

Fig. 1. Diesel engine out SO_x concentration as a function of sulfur content in diesel fuel at air/fuel mass ratios of 25–35. Diesel fuel was assumed to be fully oxidized to CO_2, H_2O and SO_x during in-cylinder combustion.

than 523 K and/or high space velocity, NO_x reduction efficiency decreases with time [6].

In this study, the effect of 50 ppmv SO_2, representative of using 1000–2000 ppmw diesel fuel, on the catalytic performance of a state-of-the-art VSCR catalyst was measured under two different types of simulated diesel engine operating conditions. One is under steady-state conditions at low temperatures from 473 to 573 K; the other is designed to simulate engine start-up and shut-down operations. The formation of ammonium sulfate species during lab reactor simulated engine start-up and shut-down and its significance are discussed.

2. Experimental

2.1. Catalyst sample

The catalyst micro-core sample is cut from the front face of the same state-of-the-art $V_2O_5/WO_3/TiO_2$ (VSCR) catalyst brick of 300 CPSI (cell per square inch) as in [11]. The catalyst sample has 12 intact monolith channels with ~6.4 mm (1/4 in.) diameter and 25.4 mm (1 in.) length. The total mass of the micro-core sample is 0.45 g.

2.2. Material characterization

Thermogravimetric analysis (TGA) was conducted on $(NH_4)_2SO_4$ (ACROS, 99%), NH_4HSO_4 (ACROS, 99%), and $(NH_4)_2SO_3{\cdot}H_2O$ (Alfa Aesar, 92%) using a TA Instruments SDT Q600. Approximately 40 mg of sample was loaded, and the temperature was then ramped to 973 K at 20 K/min under 100 sccm (standard cubic centimeters) of flowing air. N_2 adsorption experiments were conducted at 77 K to obtain the BET (Brunauer–Emmett–Teller) surface area using a Micrometrics TriStar II 3020 physisorption analyzer. The fresh micro-core catalyst was first degassed under vacuum at 623 K for 2 h; while the sulfur exposed catalyst sample was degassed at 373 K for 1 h under flowing N_2 to avoid decomposition of ammonium sulfur compounds. The diffuse reflectance Fourier transform infrared spectra were recorded with a Nicolet 6700 spectrometer with a liquid N_2 cooled MCT detector. Catalyst samples were prepared ex situ in the micro-core reactor described below, and washcoat material was scraped from the catalyst substrate for analysis. Spectra were collected at room temperature in diffuse reflectance mode by utilizing a Harrick Praying Mantis diffuse reflectance accessory purged with flowing N_2. The spectra were averaged from 64 scans at a resolution of 2 cm^{-1}. Pure KBr powder was used as the background.

2.3. Flow reactor set-up

A flow through micro-core reactor was used to characterize the catalytic performance of the VSCR catalyst. The configuration of the reactor system has been reported in a previous publication [11]. Briefly, the reactor utilizes 14 MKS mass flow controllers (MFCs) for controlling and monitoring reaction gas flow rate. The reaction gases, Ar, CO_2, O_2, 1 vol.% (volume percent) NO/Ar, 1 vol.% NH_3/Ar, 1.25 vol.% NO_2/Ar, 20 vol.% H_2/Ar, 1000 ppmv SO_2/Ar are supplied by AirGas in cylinders and are all UHP grade or higher. Water for the reaction gas is generated by reacting 20 vol.% H_2/Ar and O_2 with 5% excess in a stainless steel water generator which is loaded with 4 g 1%Pt/Al_2O_3(Sigma–Aldrich) and heated to ~430 K. The quartz reactor tubes are 22 in. long with 7 and 9.5 mm inner and outer diameters, respectively, and they are horizontally placed in a Lindberg Blue M miniMite tube furnace for reaction temperature control. Type K thermocouples (0.02 in. diameter) are placed at both ends of the catalyst bed for temperature control and measurement. The gas mixture composition, either after passing through the catalyst bed or the reactor by-pass line, is analyzed by a MKS 2030 Fourier transform infrared (FTIR) spectrometer. All the gas lines are constructed using Swagelok stainless steel tubing and heated to ~473 K to minimize adsorption of H_2O, NH_3 and SO_2.

2.4. SCR performance measurement

To simulate the diesel engine exhaust gas composition, 7 vol.% CO_2, 8 vol.% H_2O and 10 vol.% O_2 in balance Ar were always used as a baseline gas feed for reaction tests in this study unless otherwise indicated. Before catalyst testing, the VSCR micro-core was degreened (DG) at 800 K for 2 h under baseline gas to stabilize the catalyst. SCR performance measurements were conducted at 60 k h^{-1} GHSV (gas hour space velocity) by flowing 804 sccm total gas mixture under two different SCR conditions, DeNOx200 and DeNOx500. In addition to the baseline gas, the SCR reaction gases for DeNOx200 consist of 200 ppmv NO and 200 ppmv NH_3; while the SCR reaction gases for DeNOx500 consist of 450 ppmv NO, 50 ppmv NO_2 and 500 ppmv NH_3. The SO_2 oxidation over VSCR was conducted at 60 k h^{-1} under baseline gas feed with and without the presence of NO_x (450 ppmv NO and 50 ppmv NO_2) from 443 to 773 K.

2.5. Effect of SO_2

2.5.1. Effect of SO_2 under SCR condition at constant temperature

The effect of SO_2 on VSCR NO_x conversion was first studied under DeNOx200 conditions from 443 to 773 K while co-feeding 50 ppmv SO_2. Next, the long-term effect of SO_2 was investigated from 473 to 573 K under DeNOx500 conditions at 60 k h^{-1}. The 50 ppmv SO_2 was introduced into the gas mixture at 523 K for 8 h, 573 K for 4 h and 473 K for 4 h in that order. Steady-state NO_x conversion was measured from 443 to 523 K under both DeNOx200 and DeNOx500 conditions without the presence of SO_2 after each temperature hold as described above.

2.5.2. Effect of SO_2 under SCR condition with low temperature events

The effects of low temperature events (LTE) and long term SO_2 exposure were evaluated under DeNOx500 in the presence of 50 ppmv SO_2. The whole experiment has a duration of approximately 140 h. During the majority of the experiment, the catalyst was held at a constant temperature of 473 K under DeNOx500 in the presence of 50 ppmv SO_2, denoted as CTS473. Two low temperature events were conducted at ~24th hour and ~70th hour, in which the catalyst temperature was cooled down to ~317 K and then heated to 473 K in a period of ~0.5 h under the same gas feeding condition as CTS473. The steady-state catalytic performance

was measured under both DeNOx500 and DeNOx200 conditions from 443 to 523 K without the presence of SO_2 after the 1st LTE, before and after the 2nd LTE and near the end of the whole test. After the whole test, the catalyst micro-core was unloaded and the BET surface area was measured. Finally, a temperature-programmed desorption (TPD) was conducted on the same micro-core after BET surface area measurement by ramping the temperature from 355 K to 780 K at 10 K/min while flowing 536 sccm gas mixture (40 k h^{-1} GHSV) of 8 vol.% H_2O and 10 vol.% O_2 in balance Ar.

3. Kinetic analysis

The kinetic analysis was performed to understand the standard SCR reaction under DeNOx200 at temperatures below 523 K. Under this condition, all reactions other than standard SCR can be neglected for this VSCR [11]. In addition, Metkar et al. reported that internal diffusion limitations were only observed for the standard SCR reaction above 523 K for a Cu–zeolite SCR [13], which has significantly higher NO_x conversion than VSCR catalysts below 523 K [14]. External mass transfer only becomes dominant at high temperature above 673 K for the fast SCR reaction over Cu–zeolite [13]. Therefore, in this study the internal and external mass transfer effects under DeNOx200 were neglected below 523 K [5,15]. The differential equation can be derived by using the plug flow reactor model:

$$\frac{d(Fy_{NO})}{dV_{cat}} = -r \quad \leftrightarrow \quad \frac{dC_{NO}}{dV_{cat}} = -\frac{P_t}{FR}\frac{r}{T} \tag{1}$$

where y_{NO} is the molar fraction of NO; F is the total gas molar flow rate (mol s^{-1}); V_{cat} is the catalyst bed volume (m^3); r is the reaction rate per catalyst bed volume (mol s^{-1} m^{-3}); C_{NO} is the molar concentration of NO (mol m^{-3}); P_t is the total pressure (Pa); R is the ideal gas constant (8.314 J mol^{-1} K^{-1}); T is the temperature (K). The reaction rate can be assumed to have first-order dependence on NO and zero-order on NH_3 for vanadia-based SCR catalysts [5,9,10]. Therefore,

$$r = kC_{NO} \tag{2}$$

$$\frac{dC_{NO}}{dV_{cat}} = -\frac{P_t}{FR}\frac{k}{T}C_{NO} \tag{3}$$

where k is reaction rate constant (s^{-1}). By absorbing the temperature in Eq. (3) into reaction rate constant k, Eq. (3) can be rewritten as

$$\frac{dC_{NO}}{dV_{cat}} = -\frac{P_t}{FR}k'C_{NO} = -\frac{P_t}{FR}A'e^{-E'/(RT)}C_{NO} \tag{4}$$

where A' is the pre-exponential factor; E' is the apparent activation energy (J mol^{-1}). Integration of Eq. (4) yields

$$\ln(1-x) = -\frac{P_t}{FR}V_{cat}A'e^{-E'/(RT)} \tag{5}$$

where x is the NO fractional conversion. Eq. (5) can be rewritten into:

$$\ln(-\ln(1-x)) = -\frac{E'}{R}\frac{1}{T} + \ln\left(\frac{P_t}{FR}V_{cat}A'\right) \tag{6}$$

Linear fitting $1/T$ vs. $\ln(-\ln(1-x))$ can derive the apparent activation energy E' and the pre-exponential factor A', which conceptually scales with the number of catalytic sites.

4. Results

4.1. Thermal analysis of ammonium sulfur compounds

It is generally understood that ammonium (bi)sulfate species could form at low temperatures (below 573 K) during the NH_3 SCR reaction in the presence of SO_3 over VSCR catalysts. If formed, ammonium (bi)sulfate can physically cover the VSCR catalyst surface and block pores resulting in loss of catalytic performance. The thermogravimetric analysis (TGA) results of $(NH_4)_2SO_4$, NH_4HSO_4 and $(NH_4)_2SO_3{\cdot}H_2O$ are presented in Fig. 2. The TGA curves for $(NH_4)_2SO_4$ and NH_4HSO_4 are consistent with previously reported results [16]. Abrupt mass loss was observed above 700 K for both $(NH_4)_2SO_4$ and NH_4HSO_4. The differential thermal analysis (DTA) results indicate that $(NH_4)_2SO_4$ and NH_4HSO_4 start to decompose at ~550 K and fully decompose at similar temperatures of 740–750 K. Consistent with the DTA results, the differential scanning calorimetry (DSC) curves for $(NH_4)_2SO_4$ and NH_4HSO_4 also display major peaks around 740–750 K, indicating the full decomposition of $(NH_4)_2SO_4$ and NH_4HSO_4. On the other hand, the DSC curves for $(NH_4)_2SO_4$ and NH_4HSO_4 have unique low temperature peaks at ~420 and ~620 K, respectively. NH_4HSO_4 displays a DSC peak at ~420 K without having apparent mass loss, likely indicating its melting at ~420 K. While $(NH_4)_2SO_4$ displays a DSC peak at ~620 K with an apparent mass loss, indicating a partial decomposition around 620 K. Kiyoura et al. conducted a mechanistic study of $(NH_4)_2SO_4$ decomposition and showed that $(NH_4)_2SO_4$ has a complex thermal decomposition process [16]. The simplified decomposition process of $(NH_4)_2SO_4$ is shown in Eqs. (7)–(9) [17].

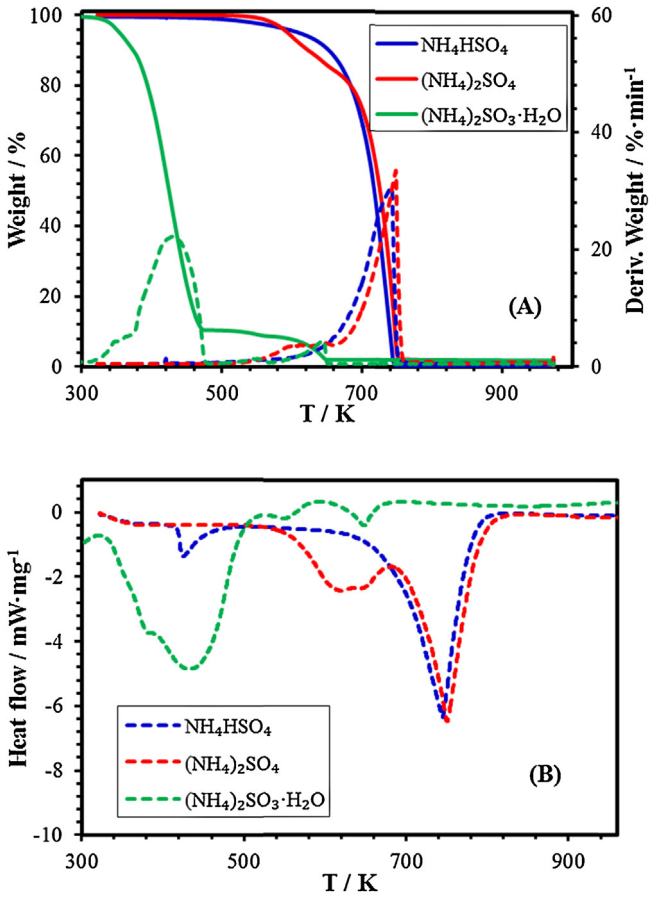

Fig. 2. (A) Thermogravimetric analysis (TGA) in solid line and differential thermal analysis (DTA) in dashed line; (B) Differential scanning calorimetry (DSC) for NH_4HSO_4, $(NH_4)_2SO_4$ and $(NH_4)_2SO_3{\cdot}H_2O$.

$$(NH_4)_2SO_4 \rightarrow NH_4HSO_4 + NH_3 \tag{7}$$

$$2NH_4HSO_4 \rightarrow (NH_4)_2S_2O_7 + H_2O \tag{8}$$

$$3(NH_4)_2S_2O_7 \rightarrow 2NH_3 + 6SO_2 + 9H_2O + 2N_2 \tag{9}$$

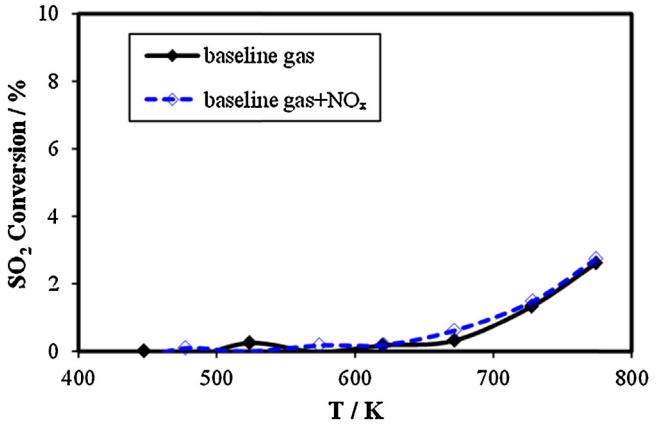

Fig. 3. SO_2 oxidation over VSCR with and without the presence of NO_x (450 ppmv NO and 50 ppmv NO_2) under baseline gas feed at 60 k h^{-1}. SO_2 Conversion = (inlet SO_2 − outlet SO_2)/inlet SO_2 × 100%.

In contrast, $(NH_4)_2SO_3{\cdot}H_2O$ starts to decompose almost from room temperature. At 470 K, 90% mass loss is observed from TGA results as shown in Fig. 2A, about 270 K lower than $(NH_4)_2SO_4$ and NH_4HSO_4. The remaining 10% mass loss for $(NH_4)_2SO_3{\cdot}H_2O$ was observed between 470 and 650 K, likely due to the impurity of this chemical.

4.2. SO_2 oxidation

Typically, commercial VSCR catalysts are optimized to minimize undesired SO_2 oxidation to SO_3 (Eq. (10)), since SO_3 can degrade catalyst performance and also lead to sulfate particulate matter emissions [8].

$$SO_2 + 0.5O_2 \leftrightarrow SO_3 \quad (10)$$

SO_2 oxidation is a reversible reaction and thermodynamically it favors SO_3 formation at low temperature. Under SCR conditions, SO_3 could react with NH_3 to form ammonium (bi)sulfate especially at low temperatures. It is reported that the activity of VSCR catalysts for SO_2 oxidation increases with vanadia loading; while the typical promoter, WO_3, increases NO_x conversion efficiency without apparently increasing SO_2 oxidation to SO_3 [18]. The SO_2 oxidation over this state-of-the-art VSCR catalyst was measured under baseline feed and the results are presented in Fig. 3. There is no apparent SO_2 conversion observed below 673 K. At 773 K, a maximum of 2.7% SO_2 conversion was observed. Since NO_2 is a stronger oxidant than O_2 and it is always present in diesel engine exhaust, its effect on SO_2 oxidation was also measured and the results are shown in Fig. 3. The presence of 50 ppmv NO_2 (500 ppmv NO_x) does not increase SO_2 conversion in comparison to conversion with the baseline gases. Thus, at the temperatures evaluated in this study, the concentration of SO_3 can be considered negligible.

4.3. NO_x conversion of VSCR

A number of reactions could occur over a VSCR catalyst in the presence of NH_3 and NO_x. A few main reactions are listed below:

$$4NH_3 + 4NO + O_2 \rightarrow 4N_2 + 6H_2O \quad (11)$$

$$2NH_3 + NO + NO_2 \rightarrow 2N_2 + 3H_2O \quad (12)$$

$$2NH_3 + 1.5O_2 \rightarrow N_2 + 3H_2O \quad (13)$$

$$NO + 0.5O_2 \leftrightarrow NO_2 \quad (14)$$

Eq. (11) is the standard SCR reaction. With the presence of NO_2 at NO_2/NO_x molar ratio close to 0.5, the fast SCR reaction (Eq. (12)) could become dominant [19]. Typical diesel engine out NO_2/NO_x molar ratio is approximately 0.1, and VSCR catalysts are not conventionally used after a diesel oxidation catalyst. Therefore, the standard SCR reaction is the primary NO_x reduction pathway over VSCR catalysts with some fast SCR reaction primarily resulting from combustion derived NO_2. Due to the oxidative nature of vanadia species, VSCR catalysts can catalyze undesired NH_3 oxidation to N_2 (above 623 K) or NO_x (above 723 K). The reversible NO oxidation (Eq. (14)) can also be catalyzed by VSCR, though the production of NO_2 is low at the temperatures evaluated in this study [11].

The steady-state NO_x conversion of this state-of-the-art VSCR catalyst at a GHSV of 60 k h^{-1} under simulated diesel exhaust conditions was measured and the results are displayed in Fig. 4A. Under DeNOx200 conditions, the NO_x conversion of DG VSCR increased from 11.4% to nearly 90% when the temperature increased from 443 to 573 K. The NO_x conversion is near or above 90% from 573 to 723 K. An apparent decrease in NO_x conversion was observed above 723 K. The decrease in NO_x conversion can be attributed to the increasing reaction rate of NH_3 oxidation at high temperature, leading to a lack of NH_3 for the SCR reaction [11,12,14]. Under DeNOx500 conditions, the NO_x conversion has a similar profile to that of DeNOx200. Below 473 K, the NO_x conversion under DeNOx500 is higher than that under DeNOx200 due to the portion of fast SCR under DeNOx500 conditions.

4.4. Effect of SO_2

The effect of SO_2 on the SCR reaction was first investigated by co-feeding SO_2 under DeNOx200 conditions from 443 to 773 K. SO_2 leads to a slight increase in NO_x conversion below 523 K. Because ammonium (bi)sulfate could possibly form in the low temperature region under SCR conditions, the low temperature exposure of SO_2 was further explored under DeNOx500, a more representative diesel exhaust condition. The VSCR catalyst was held under DeNOx500, while co-feeding 50 ppmv SO_2, at 523 K for 8 h, at 573 K for 4 h, and then at 473 K for 4 h. Catalytic performance was measured under DeNOx200 and DeNOx500 from 443 to 523 K without the presence of SO_2 after each temperature hold. The results are illustrated in Fig. 4A and B. NO_x conversion for both DeNOx200 and DeNOx500 slightly increases with each SO_2 exposure at 523, 573 and 473 K in sequence.

The kinetic analysis results of DeNOx200 with and without SO_2 and with exposure to SO_2 at 523, 573 and 473 K are shown in Fig. 4C and D. The DG VSCR has apparent activation energy of 55.5 kJ/mol for the standard SCR reaction. Co-feeding SO_2 under DeNOx200 conditions does not affect the apparent activation energy, but the pre-exponential factor increases 9%. Similarly, upon exposure of this VSCR catalyst to 50 ppmv SO_2 at 523, 573 and 473 K for several hours, the apparent activation energy stays constant in the range of 54.5–56.5 kJ/mol. However, the pre-exponential factor increases 20–33% relative to that of the DG VSCR catalyst as shown in Fig. 4D.

In actual diesel aftertreatment operation, the aftertreatment catalyst will be exposed to much lower temperatures than 473 K, such as ambient temperature during engine start-up and shutdown. To simulate these conditions, a long term SO_2 exposure under DeNOx500 at 473 K was conducted with low temperature events. NO_x conversion over the entire 140 h experiment is illustrated in Fig. 5A. From 11 to 21 h, the VSCR catalyst was held at 473 K under DeNOx500 condition in the presence of 50 ppmv SO_2. It can be seen that the NO_x conversion remains constant at ~34.5% throughout this 10 h period. At time ~24 h, the 1st low temperature event was conducted by rapidly cooling the catalyst temperature to ~317 K then heating to 473 K over the period of half an hour without changing gas flow conditions. As seen in Fig. 5A, when the

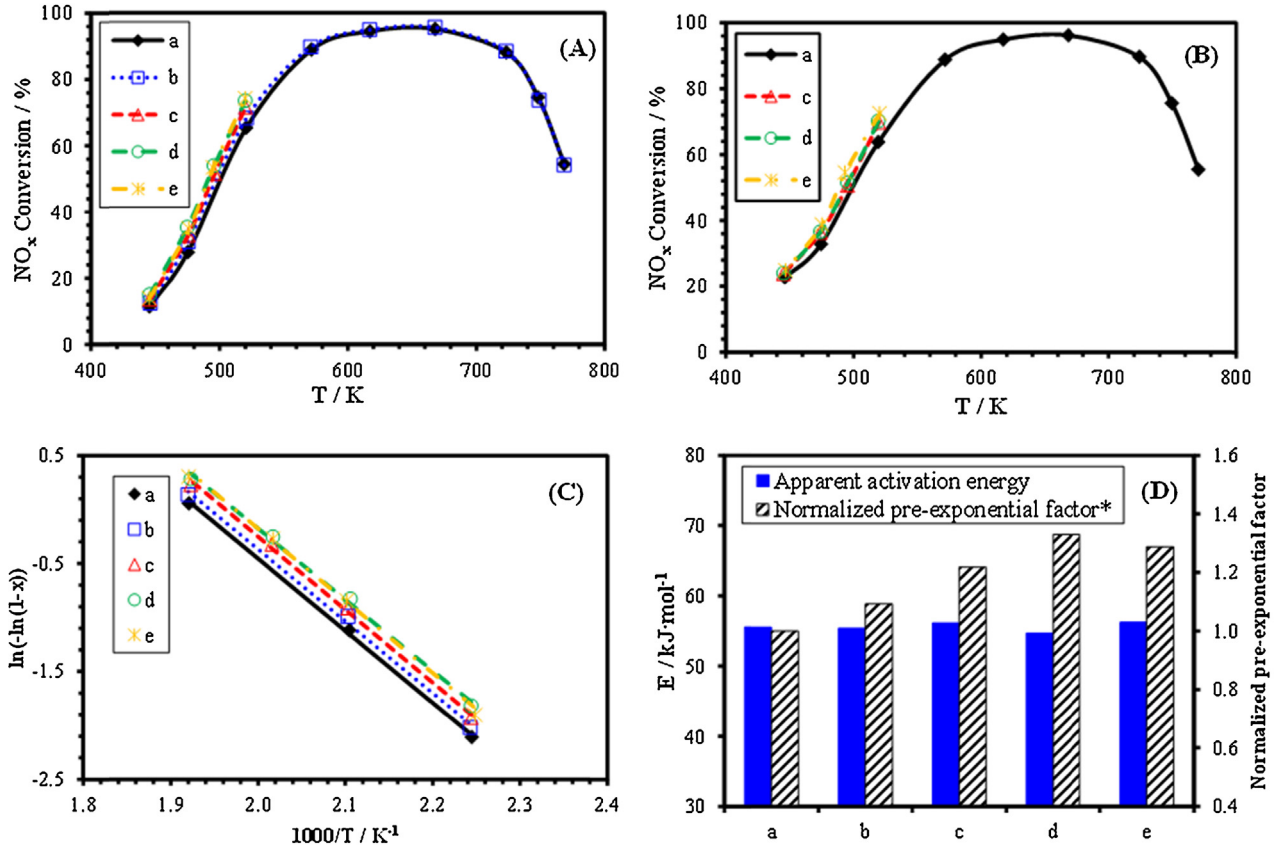

Fig. 4. (A) NO_x conversion under DeNOx200; (B) NO_x conversion under DeNOx500; (C) kinetic analysis for DeNOx200 below 523 K; (D) apparent activation energy and normalized pre-exponential factors relative to DG VSCR. (a) DG VSCR; (b) DeNOx200 with co-feeding 50 ppmv SO_2; (c) 50 ppmv SO_2 exposure under DeNOx500 at 523 K for 8 h; (d) 50 ppmv SO_2 exposure under DeNOx500 at 523 K for 8 h + 573 K for 4 h; (e) 50 ppmv SO_2 exposure under DeNOx500 at 523 K for 8 h + 573 K for 4 h + 473 K for 4 h. *The pre-exponential factor was calculated by fixing the apparent activation energy at the averaged value from a to e.

temperature returned to 473 K, the NO_x conversion instantaneously dropped approximately 5% in comparison to conversion before the 1st low temperature event. After the 1st low temperature event, the NO_x conversion continuously decreases with additional exposure of this VSCR catalyst at 473 K to 50 ppmv SO_2 under DeNOx500 conditions. Overall, a 15% decrease in NO_x conversion is observed at time ~140 h, in comparison to NO_x conversion before the 1st low temperature event. A 2nd low temperature event was also conducted at 70 h. In comparison to the 1st low temperature event, no apparent NO_x conversion drop was observed after the 2nd low temperature event. The steady-state NO_x conversion performance of this VSCR was measured from 443–523 K for both DeNOx200 and DeNOx500 without the presence of SO_2 at time points P (27–31 h), Q (65–68 h), R (75–79 h) and S (129–133 h) as shown in Fig. 5A. The results are illustrated in Fig. 6A and B. The steady-state NO_x conversion from 443–523 K for both DeNOx200 and DeNOx500 decreases significantly upon long term SO_2 exposure after low temperature events. By time S, the NO_x conversion has dropped 40% for DeNOx200 and 30% for DeNOx500 at 523 K. The kinetic analysis was conducted for DeNOx200 at points P, Q, R and S and the results are illustrated in Fig. 6C and D. The standard SCR apparent activation energies at points P, Q, R and S are relatively constant in the range of 52.6–57.6 kJ/mol, similar to the DG VSCR value of 55.5 kJ/mol. On the other hand, the normalized pre-exponential factors at points P, Q, R and S decrease substantially relative to DG VSCR. At point S, after ~106 h of CTS473 and two low temperature events, the pre-exponential factor dropped to less than 30% of the DG VSCR catalyst as shown in Fig. 6D. The nearly constant apparent activation energy and the reduction in pre-exponential factor during the long term CTS473 with low temperature events indicate that the nature of VSCR catalytic sites remains relatively unchanged while the number of catalytic sites declines significantly.

The concentrations of gas phase species and the temperature profile during the 1st low temperature event are displayed in Fig. 5B and C. As the temperature cools, the concentrations of both NO and NO_2 increase because of the lower SCR reaction rate at decreased temperature. While NH_3 concentration initially drops, due to increased NH_3 adsorption onto the VSCR catalyst at decreased temperature; it then increases because of the lower SCR reaction rate. The concentration of SO_2 starts to decrease at 423 K and is almost zero below 373 K. Water concentration also decreases slightly with a maximum 0.5% change at the lowest temperature point of 317 K as shown in Fig. 5C. Small liquid drops were observed on the inner side of the quartz reactor wall when temperature was decreased below ~323 K. When temperature increases from 317 to 473 K, a small water peak, reaching 9.1%, at 321 K was first observed. This was followed by NH_3, NO and NO_2 peaks, significantly higher than their feeding concentrations, appearing at almost the same temperatures of 330–335 K, likely due to the portion of these gases dissolved into condensed liquid. A small peak of N_2O with a maximum less than 4 ppmv was observed at ~400 K, likely indicating ammonium nitrate formation during low temperature events [14,19]. Then a second peak for NO_2 and NH_3, again both greater than their feeding concentrations, appears at ~460 and ~470 K, respectively, presumably from the physically adsorbed portion on the catalyst when the temperature cools down. The SO_2 concentration starts to increase at ~373 K from almost zero and reaches the feeding concentration above 440 K. It is worth pointing out that no apparent SO_2 peak above the feeding concentration of 50 ppmv was observed as the temperature returned to 473 K. After

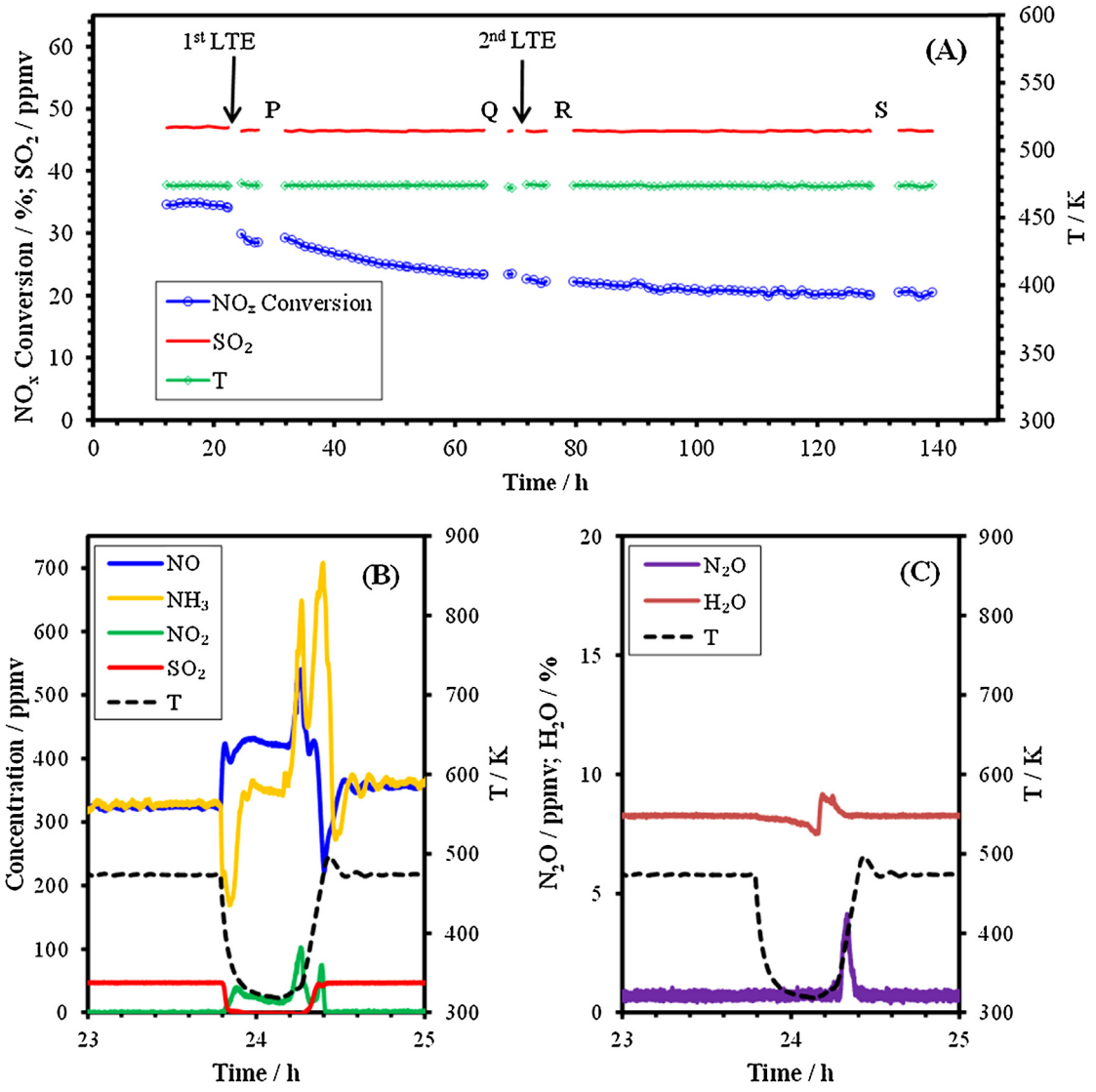

Fig. 5. (A) NO_x conversion at 473 K under DeNOx500 in the presence of 50 ppmv SO_2 with two low temperature events at 24 h and 70 h. Catalytic performance was measured at time points P, Q, R and S under DeNOx200 and DeNOx500 from 443 to 523 K without the presence of SO_2; (B) NO, NH_3, NO_2, SO_2 concentration and temperature profile during 1st low temperature event; (C) N_2O and H_2O concentration and temperature profile during 1st low temperature event.

the temperature is stabilized at 473 K, the outlet NO_x concentration has increased from 325 ppmv before the event to 354 ppmv. Thus, as previously mentioned, the 1st low temperature event caused a ~5% NO_x conversion decrease.

After the 140 h test with low temperature events, the catalyst was unloaded. Small crystallite substances were observed on the inner side of the quartz reactor wall. On the contrary, no crystals were observed after the SO_2 exposure tests with temperature holds at 523, 573 and 473 K. The catalyst was degassed under N_2 flow for 1 h at 373 K, and BET surface area was measured. It reveals ~40% surface area loss after long term CTS473 with two low temperature events. After the BET surface area measurement, the catalyst was loaded into a clean quartz reactor and a TPD experiment was performed. The gas species release profile is shown in Fig. 7. A significant amount of SO_2 release was observed. The SO_2 starts to release from the catalyst at 630 K, peaks at 695 K, and decreases substantially above 750 K. The sulfur loading was estimated to be 30 μmol/g_cat by integrating the measured SO_2 concentration over time during the TPD experiment. NH_3 starts to release at a much lower temperature of 480 K with a major broad peak from 530 to 580 K and a wide shoulder from 630 to 750 K overlapping with the SO_2 release. The total NH_3 uptake was calculated to be 180 μmol/g_cat. On the other hand, the release of CO_2, NO_x and N_2O is negligible during the TPD experiment as shown in Fig. 7.

Infrared spectra of DG VSCR and VSCR after one low temperature event (VSCR with LTE) are displayed in Fig. 8. VSCR with LTE was prepared ex situ in the micro-core reactor. After degreening, the catalyst was exposed to 50 ppmv SO_2 under DeNOx500 at 473 K for ~12 h, one LTE and an additional ~24 h exposure of 50 ppmv SO_2 under DeNOx500 at 473 K. In comparison to DG VSCR, VSCR with LTE shows enhanced IR absorption at 980, 1050, 1140 and 1210 cm^{-1}, which were previously observed on sulfated V_2O_5–WO_3/TiO_2 catalysts [20] and sulfated titania materials [28]. It was also reported that $(NH_4)_2SO_4$ has $\nu_4(SO_4^{2-})$ mode IR absorption at 1050 and 1150 cm^{-1} and $\nu_1(SO_4^{2-})$ mode at 952 and 982 cm^{-1} [21]. Therefore, the increased IR absorption at 980, 1050, 1140 and 1210 cm^{-1} on VSCR with LTE indicates the accumulation of sulfate species onto VSCR catalyst surfaces as a result of the LTE and the further 50 ppmv SO_2 treatment under DeNOx500 at 473 K. In addition, a broad absorption band from 1380 to 1500 cm^{-1} with a peak at 1435 cm^{-1} and two shoulders at 1400 and 1470 cm^{-1}, was also observed for VSCR with LTE as shown in Fig. 8. This absorption

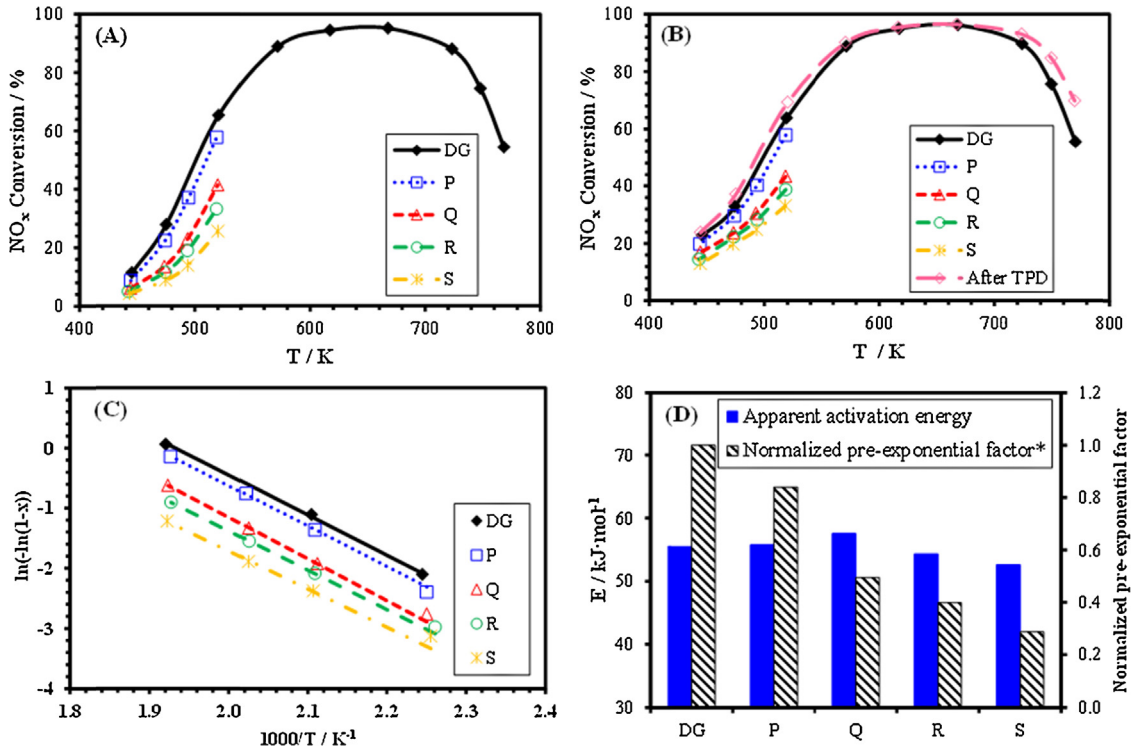

Fig. 6. (A) NO_x conversion under DeNOx200; (B) NO_x conversion under DeNOx500; (C) kinetic analysis for DeNOx200 below 523 K; (D) apparent activation energy and normalized pre-exponential factor relative to that of DG VSCR. *The pre-exponential factor was calculated by fixing the apparent activation energy at the averaged value from DG, P, Q, R and S.

band can be attributed to the vibration frequency of chemically adsorbed NH_3 on the Brönsted acidic sites of VSCR catalysts from 1415 to 1460 cm^{-1} [5,23,24,28] and the NH_4^+ vibration of ammonium sulfate species, such as ammonium bisulfate and ammonium sulfate, at 1410 cm^{-1} [22].

After exposure at 773 K during the TPD experiment, the catalytic performance of this VSCR was further tested under DeNOx500 conditions and the results are in Fig. 6B. The NO_x conversion was fully recovered with a slight increase in comparison to the DG VSCR, presumably due to the increased number of Brönsted acidic sites upon long term SO_2 exposure. The full recovery of NO_x reduction performance indicates that the ammonium sulfate species deposited as a result of low temperature events completely decompose during the TPD experiment.

5. Discussion

Typically, commercial VSCR catalysts consist of approximately 1–3 wt.% vanadium oxide supported on anatase phase titanium dioxide with about 10 wt.% tungsten oxide as a promoter to improve the Brönsted acidity [11,27]. The vanadia component has dual functionality of providing Brönsted acidity and redox sites; both play important roles for the SCR reaction [24–27]. The loading of vanadia is optimized to provide high NO_x conversion efficiency while minimizing its oxidation reactivity for NH_3 and SO_2 oxidation. Fig. 3 shows that this state-of-the-art VSCR does not oxidize SO_2 below 673 K with or without the presence of NO_x (450 ppmv NO and 50 ppmv NO_2). However, the interaction between SO_2 and the VSCR catalyst surface below 673 K cannot be excluded. Sulfate species were detected on TiO_2 under SCR conditions and in the presence of SO_2 using thermogravimetric analysis and X-ray photoelectron spectroscopy [28,29], and it has previously been shown that the formation of SO_2 derived surface sulfate species on VSCR catalysts can lead to increased Brönsted acidity which facilitates the adsorption and activation of NH_3 and hence increases the SCR reaction rate and the NO_x conversion [5,9,10,31]. In agreement with these previous studies, the results from this work also show that co-feeding 50 ppmv SO_2 under SCR conditions results in increased NO_x conversion. The kinetic analysis results in Fig. 4C and D shows that the apparent activation energy remains constant during the SO_2 exposure under SCR conditions while the pre-exponential factor increases. This is consistent with the results recently reported by Guo et al. that pretreatment of 5 wt.% V_2O_5/TiO_2 with 2700 ppmv SO_2 at 653 K for 0.5–24 h shows constant activation energy with increased pre-exponential factor [5]. Infrared spectroscopy characterization of 5 wt.% V_2O_5/TiO_2 upon SO_2 treatment indicates increased number of Brönsted acidic sites without changing the acidic strength of the sites [5]. Chen and Yang [10] also observed that the standard SCR reaction rate constant is 23% higher in the presence of 1000 ppmv SO_2 at 573 K for a 5% V_2O_5/TiO_2 catalyst than without the presence of SO_2. On the other hand, exposure of vanadia SCR catalysts to SO_2 could also lead to ammonium (bi)sulfate formation under certain conditions. Magnusson et al. studied the effect of several hundred ppmv of SO_2 on a vanadia SCR catalyst for marine application. It was found that no apparent deactivation was observed when co-feeding 500 ppmv SO_2 under SCR conditions above 573 K and at low SV of 12 k h^{-1}. However, at a lower temperature of 523 K and higher SV of 18.3 k h^{-1}, a continuous decrease in NO_x conversion was observed and the formation of ammonium sulfate was proposed to be the cause [6]. Because of these opposite effects of SO_2, i.e. increasing reactivity due to increasing number of Brönsted acidic sites or decreasing reactivity due to formation of ammonium (bi)sulfate which blocks VSCR active sites, the overall effect of SO_2 will depend on the operating conditions. Low temperature and high SO_2 concentration are prone to result in VSCR deactivation due to ammonium (bi)sulfate formation. At high temperature, above 573 K, in the presence of SO_2 under SCR conditions, any formed ammonium (bi)sulfate tends to decompose. Therefore the promotional effect of SO_2 will become dominant. In this study, a slight increase in NO_x conversion was

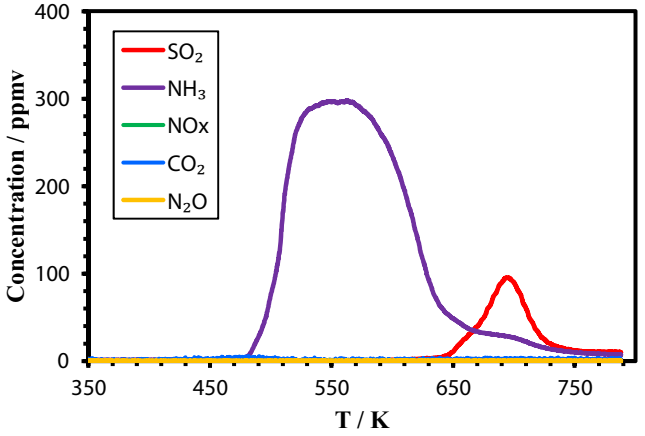

Fig. 7. Gas species release profile for SO_2, NH_3, CO_2, NO_x, and N_2O upon temperature-programmed desorption of VSCR catalyst sample after 140 h CTS473 experiment with low temperature events in Fig. 5A.

observed after co-feeding 50 ppmv SO_2 under SCR conditions from 473 to 573 K for 4–8 h as shown in Fig. 4A and B.

In actual diesel aftertreatment applications, the catalyst will be exposed to exhaust at much lower temperatures during engine start-up and shut-down than the temperatures previously evaluated in lab reactor experiments, typically above 423 K [5,9,10,29,30]. To simulate engine start-up or shut-down, the long term CTS473 was conducted with low temperature events and the results are shown in Fig. 5A. From 11 to 21 h, the NO_x conversion remains constant at ~34.5% when co-feeding 50 ppmv SO_2 under DeNOx500 at a constant temperature of 473 K. The effect of low temperature events is significant. After the 1st low temperature event, the NO_x conversion dropped ~5% at 473 K. Furthermore, additional constant temperature SO_2 exposure at 473 K after the 1st low temperature event leads to further catalyst deactivation (25–65 h in Fig. 5A). A controlled experiment was conducted to exclude the possibility that these findings could be due to the formation of ammonium (bi)carbonate and/or ammonium nitrate during the low temperature event. The experiment was conducted by cooling the temperature from 473 K to ~317 K under DeNOx500 without the presence of SO_2 then heating back to 473 K and holding for more than 10 h. NO_x conversion at 473 K was constant before and after this low temperature event. Therefore, the detrimental effect of the 1st low temperature event is not due to ammonium (bi)carbonate and/or ammonium nitrate formation. When the temperature is decreased below 373 K during the low temperature event, SO_2 concentration drops almost to zero as shown in Fig. 5B. When the temperature approaches a minimum at 23.9–24.2 h in Fig. 5B, the concentrations of all gas species approach a "steady" state. It is notable that the total NO_x concentration is about 90 ppmv higher than NH_3. The diminished NH_3 is likely reacting with SO_2 in an approximately 2:1 molar ratio forming ammonium sulfite which indiscriminately deposits on both the catalyst surface and the inner quartz reactor wall. To further confirm the reaction between SO_2 and NH_3, another controlled experiment was conducted by cooling the temperature under the same conditions as Fig. 5A except without feeding NO_x and NH_3; SO_2 concentration decreased less than 3 ppmv at the lowest temperature of ~317 K, confirming the interaction between NH_3 and SO_2 below 373 K.

As it is displayed in Fig. 2A, ammonium sulfite decomposes below 470 K. However, during the process of increasing the temperature to 473 K, no apparent SO_2 peak above 50 ppmv was observed and NO_x conversion decreased ~5% when temperature stabilized at 473 K as shown in Fig. 5A and B. Thus, the ammonium sulfite formed during the low temperature event is likely oxidized to ammonium

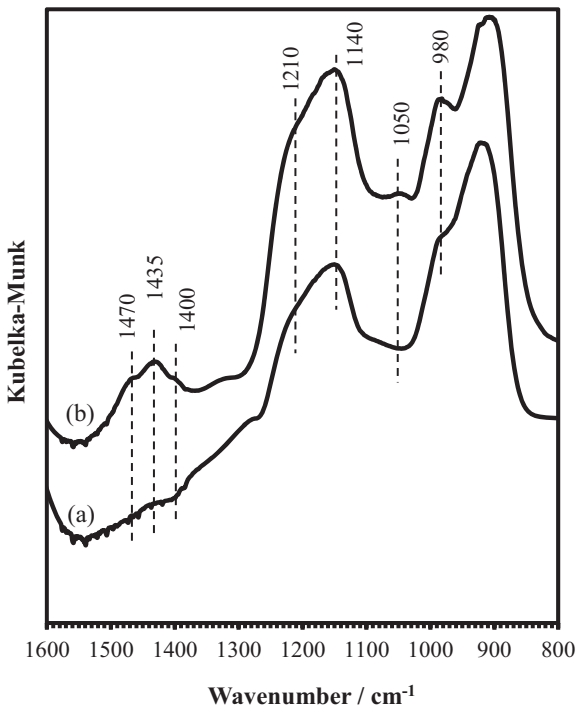

Fig. 8. Diffuse reflectance infrared Fourier transform spectra (DRIFTS) of solid samples: (a) DG VSCR; (b) VSCR with LTE, i.e., 50 ppmv SO_2 exposure under DeNOx500 at 473 K for ~12 h + one LTE + additional ~24 h exposure of 50 ppmv SO_2 under DeNOx500 at 473 K.

sulfate species, such as $(NH_4)_2SO_4$, NH_4HSO_4 or $(NH_4)_2S_2O_7$. As previously shown by the TGA results in Fig. 2, these new ammonium sulfur species are significantly more refractory than ammonium sulfite. This hypothesis is confirmed by the high temperature SO_2 release peak at ~695 K during the TPD experiment as shown in Fig. 7. The observed IR absorption bands at 980, 1050, 1140 and 1210 cm^{-1} associated with sulfate species and the IR absorption from 1380 to 1500 cm^{-1} due to ammonia species on VSCR with LTE in Fig. 8 further confirm the formation of ammonium sulfate species during LTE and the further 50 ppmv SO_2 treatment under DeNOx500 condition at 473 K. As was previously mentioned, liquid drop formation was visually observed on the inner wall of the quartz reactor during low temperature events below 323 K and crystallite substances were observed on the reactor tube after the 140 h test in Fig. 5A. These crystallite substances are apparently more stable than ammonium sulfite species which decomposed below 470 K as shown in Fig. 2A since they were still present after exposure to 523 K during catalytic performance evaluation in point R and S in Fig. 5A. It is likely that the ammonium sulfite species in the liquid drops were oxidized to ammonium sulfate species during low temperature events and that this process does not require a catalyst. Indeed, it was reported that ammonium sulfite solution can be easily oxidized by the oxygen in air to ammonium sulfate during the flue gas scrubbing process of fertilizer production [32]. In addition, gas phase NO and NO_2 can be absorbed into ammonium (bi)sulfite solution, and the co-presence of NO and NO_2 could increase the absorption of each other at 403 K [33]. It was also reported that in the presence of oxygen, the absorption of NO_2 could enhance the oxidation of sulfite [34,35]. The NO and NO_2 release measured upon heating after the 1st low temperature event (Fig. 5B) indicate that their presence in solution may be aiding the oxidation of ammonium sulfite species.

In addition to the instantaneous reduction in NO_x conversion, the 1st low temperature event also leads to a decline in NO_x conversion that continues throughout the CTS473 experiment as shown

in Fig. 5A. It is known that ammonium sulfate species are sticky and acidic [36]. Once formed on the catalyst surface during a low temperature event, these species may continue to adsorb NH_3 and SO_2 at 473 K, temporarily forming ammonium sulfite species, which are likely then further oxidized to ammonium sulfate species. What begin as "islands" of ammonium sulfate formed on the catalyst surface after the low temperature event, slowly expand and cover additional catalyst sites with continued exposure to NH_3 and SO_2 at 473 K. The TPD results shown in Fig. 8 indicate a significant amount of NH_3 uptake onto the VSCR catalyst after the 140 h CTS473 experiment. The total NH_3 uptake is estimated to be about 80% higher than the NH_3 storage at 473 K in [11]. The significantly increased NH_3 uptake can be attributed to the formation of ammonium sulfate species and NH_3 adsorption on formed ammonium sulfate species due to its acidic nature [36]. Based on the TGA and DSC results from Fig. 2, these ammonium sulfate species can partially decompose below 630 K [16], likely forming NH_4HSO_4 and/or $(NH_4)_2S_2O_7$ as shown in Eq. (8) and Eq. (9) [17]. Therefore the NH_3 release in Fig. 7 below 630 K can be attributed to the release of adsorbed NH_3 on the acidic sites of VSCR catalyst and acidic ammonium sulfate species and to the partial decomposition of formed ammonium sulfate species. Above 665 K, the NH_3 release concentration is lower than that of SO_2 as shown in Fig. 7. At the peak SO_2 release temperature of 695 K, the NH_3 release concentration is approximately 1/3 of SO_2, likely indicating that the decomposition path follows Eq. (9) which could result in an NH_3/SO_2 molar ratio of 1:3.

6. Conclusions

The influence of 50 ppmv SO_2 on a state-of-the-art VSCR was investigated under two different types of simulated diesel engine operating conditions. Under constant temperature SO_2 exposure from 473 to 573 K for 4–8 h, the NO_x conversion was slightly improved. Kinetic analysis under DeNOx200 at temperatures below 523 K indicates a small increase of pre-exponential factor while the apparent activation energy remains constant. On the other hand, the 1st low temperature event simulating engine start-up and shut-down in the presence of 50 ppmv SO_2 leads to an instantaneous drop of 5% NO_x conversion at 473 K under DeNOx500 conditions. Further degradation of NO_x conversion after the low temperature event was observed in the presence of 50 ppmv SO_2 under DeNOx500 at 473 K. Both the SO_2 release at 695 K from the TPD experiment and the IR absorption bands associated with sulfate and ammonia species indicate the formation of ammonium sulfate species. In addition, reductions in BET surface area and pre-exponential factor from kinetic analysis confirmed that reductions in NO_x conversion are due to physical poisoning of the VSCR catalyst. This work illustrates that SO_2 and NH_3 can combine and further be oxidized to ammonium sulfate species during low temperature events simulating engine start-up and shut-down processes, and that the ammonium sulfate species formed during the low temperature event make the VSCR catalyst susceptible to further degradation by SO_2 at 473 K.

Acknowledgements

The authors would like to acknowledge Dr. Aleksey Yezerets and Mr. Neal W. Currier from Cummins Inc. for their invaluable suggestions. The authors would also like to acknowledge Dr. Xu Chen and Dr. Matthew Henrichsen from Cummins Inc. for their technical discussion. The authors are grateful to Dr. Hongmei An and Mr. David D. Klippstein from Cummins Inc. for their assistance with thermal analysis experiments and Dr. Jinyong Luo and Mr. Randall P. Jines from Cummins Inc. for their assistance with IR experiments.

References

[1] Z.G. Liu, N.A. Ottinger, C.M. Cremeens, SAE Int. J. Engines. 5 (2012) 663–671.
[2] S. Matsuda, T. Kamo, A. Kato, F. Nakajlma, T. Kumura, H. Kuroda, Ind. Eng. Chem. Prod. Res. Dev. 21 (1982) 48–52.
[3] E. Tronconi, A. Cavanna, C. Orsenigo, P. Forzatti, Ind. Eng. Chem. Res. 38 (1999) 2593–2598.
[4] J.P. Dunn, H.G. Stenger, I.E. Wachs, J. Catal. 181 (1999) 233–243.
[5] X. Guo, C. Bartholomew, W. Hecker, L.L. Baxter, Appl. Catal. B-Environ. 92 (2009) 30–40.
[6] M. Magnusson, E. Fridell, H.H. Ingelsten, Appl. Catal. B-Environ. 111/112 (2012) 20–26.
[7] N.J. Khatri, J.H., Johnson, D.G. Leddy, SAE Paper no. 780111.
[8] J.C. Wall, S.K. Hoekman, SAE Paper no. 841364.
[9] M.D. Amiridis, I.E. Wachs, G. Deo, J.M. Jehng, D.S. Kim, J. Catal. 161 (1996) 247–253.
[10] J.P. Chen, R.T. Yang, J. Catal. 125 (1990) 411–420.
[11] Y. Xi, N.A., Ottinger, Z.G. Liu, SAE Paper no. 2013-01-1079.
[12] M.P. Ruggeri, I. Nova, E. Tronconi, Chem. Eng. J 207/208 (2012) 57–65.
[13] P.S. Metkar, V. Balakotaiah, M.P. Harold, Chem. Eng. Sci. 66 (2011) 5192–5203.
[14] K. Kamasamudram, N.W. Currier, X. Chen, A. Yezerets, Catal. Today 151 (2010) 212–222.
[15] L. Olsson, H. Sjovall, R.J. Blint, Appl. Catal. B-Environ. 81 (2008) 203–217.
[16] R. Kiyoura, K. Urano, Ind. Eng. Chem. Process Des. Develop. 9 (1970) 489–494.
[17] Y. Liske, S. Kapila, V. Flanigan, P. Nam, S. Lorbert, J. Hazard. Subst. Res. 2 (2000) 1–17.
[18] J.P. Dunn, P.R. Koppula, H.G. Stenger, I.E. Wachs, Appl. Catal. B-Environ. 19 (1998) 103–117.
[19] M. Koebel, G. Madia, M. Elsener, Catal. Today 73 (2002) 239–247.
[20] C. Orsenigo, L. Lietti, E. Tronconi, P. Forzatti, F. Bregani, Ind. Eng. Chem. Res. 37 (1998) 2350–2359.
[21] T.J. Fortin, J.E. Shilling, M.A. Tolbert, J. Geophys. Res. 107 (2002), AAC 4-1–AAC 4-9.
[22] F.A. Miller, C.H. Wilkins, Anal. Chem. 24 (1952) 1253–1294.
[23] D. Nicosia, M. Elsener, O. Krocher, P. Jansohn, Top. Catal. 42/43 (2007) 333–336.
[24] N.Y. Topsøe, H. Topsoe, J.A. Dumesic, J. Catal. 151 (1995) 226–240.
[25] N.Y. Topsøe, J.A. Dumesic, H. Topsoe, J. Catal. 151 (1995) 241–252.
[26] J.A. Dumesic, N.Y. Topsøe, H. Topsøe, Y. Chen, T. Slabiaky, J. Catal. 163 (1996) 409–417.
[27] I.E. Wachs, G. Deo, B.M. Weckhuysen, A. Andreini, M.A. Vuurman, M. de Boer, M.D. Amiridisz, J. Catal. 161 (1996) 211–221.
[28] J.P. Chen, R.T. Yang, J. Catal. 139 (1993) 277–288.
[29] S.T. Choo, Y.G. Lee, I.S. Nam, S.W. Ham, J.B. Lee, Appl. Catal. A-Gen. 200 (2000) 177–188.
[30] I. Nova, C. Ciardelli, E. Tronconi, D. Chatterjee, B. Bandl-Konrad, AIChE J. 52 (2006) 3222–3233.
[31] M. Kobayashi, M. Hagi, Appl. Catal. B-Environ. 63 (2006) 104–113.
[32] J. Zhou, W. Li, W. Xiao, Chem. Eng. Sci. 55 (2000) 5637–5641.
[33] X. Gao, Z. Du, H. Ding, Z. Wu, H. Lu, Z. Luo, K. Cen, Fuel Process. Technol. 92 (2011) 1506–1512.
[34] D. Littlejohn, Y.Z. Wang, S.G. Chang, Environ. Sci. Technol. 27 (1993) 2162–2167.
[35] C.H. Shen, G.T. Rochelle, Environ. Sci. Technol. 32 (1998) 1994–2003.
[36] J. Menasha, D. Dunn-Rankin, L. Muzio, J. Stallings, Fuel 90 (2011) 2445–2453.